

## Pre-organisation of ligand donor sets modulates the supramolecular structure of bis(pyridyl-imine) silver(I) chelates

Chané Venter and Matthew P. Akerman\*

School of Chemistry and Physics, University of KwaZulu-Natal, Private Bag X01, Scottsville,  
Pietermaritzburg, 3209, South Africa

E-mail: [akermanm@ukzn.ac.za](mailto:akermanm@ukzn.ac.za)

Tel: +27(0)33 260 5293

Fax: +27(0)33 260 5009

### Electronic Supplementary Information

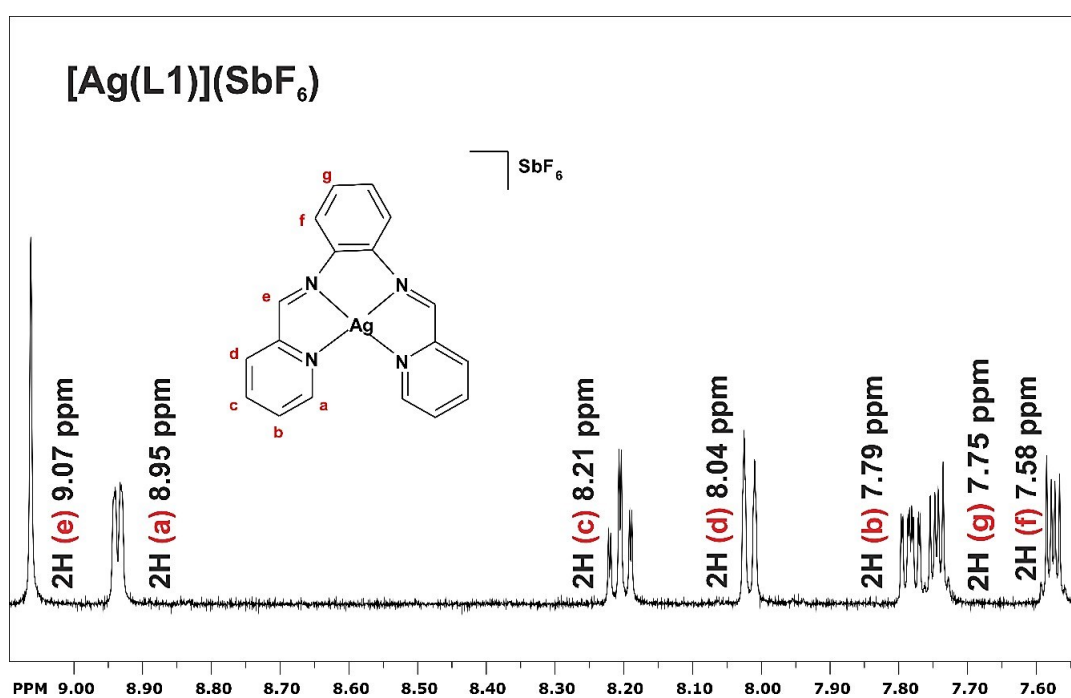
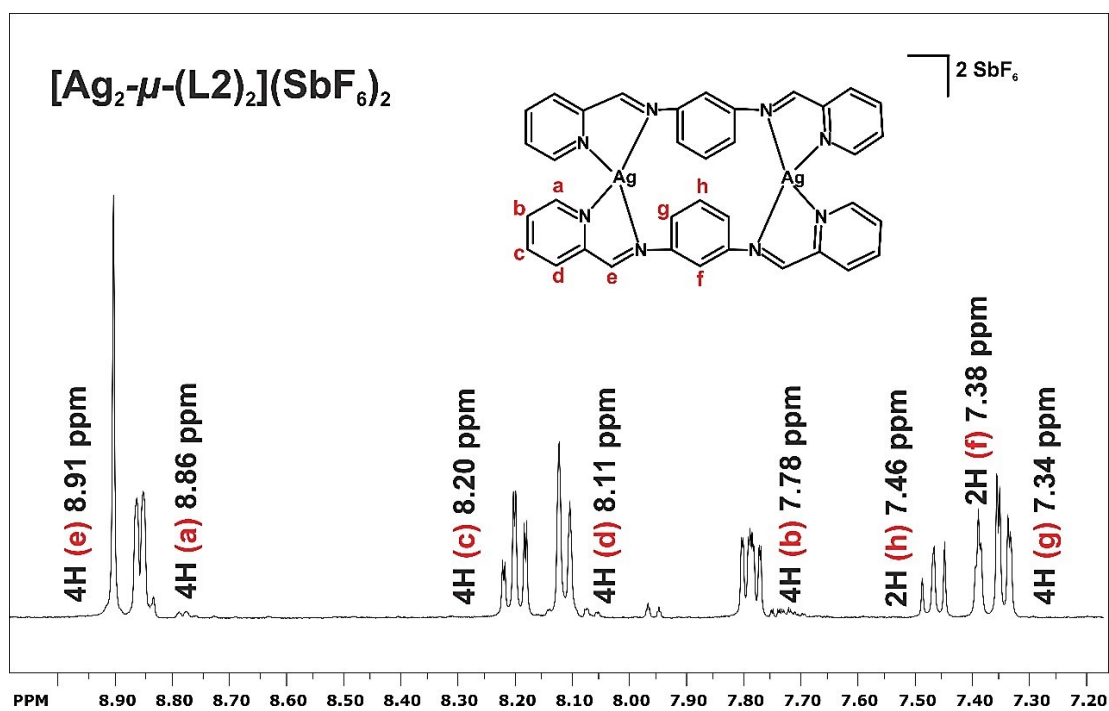
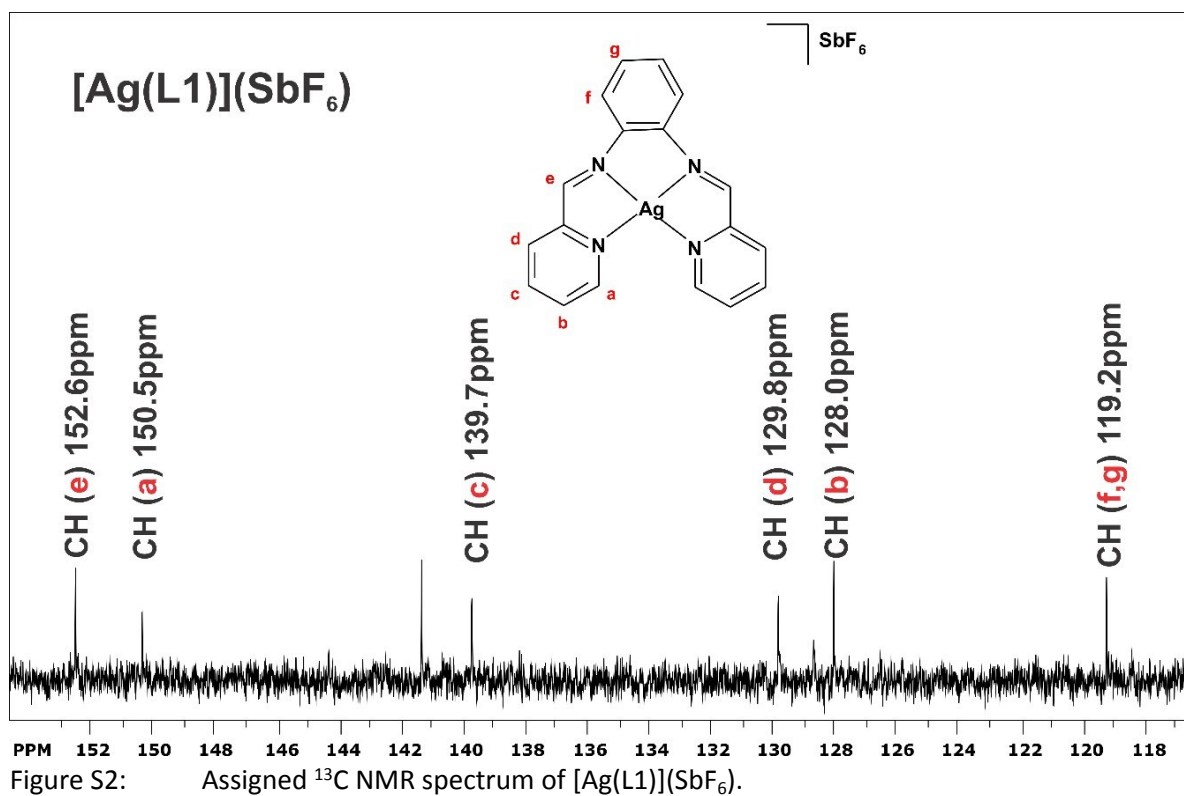


Figure S1: Assigned <sup>1</sup>H NMR spectrum of [Ag(L1)](SbF<sub>6</sub>).



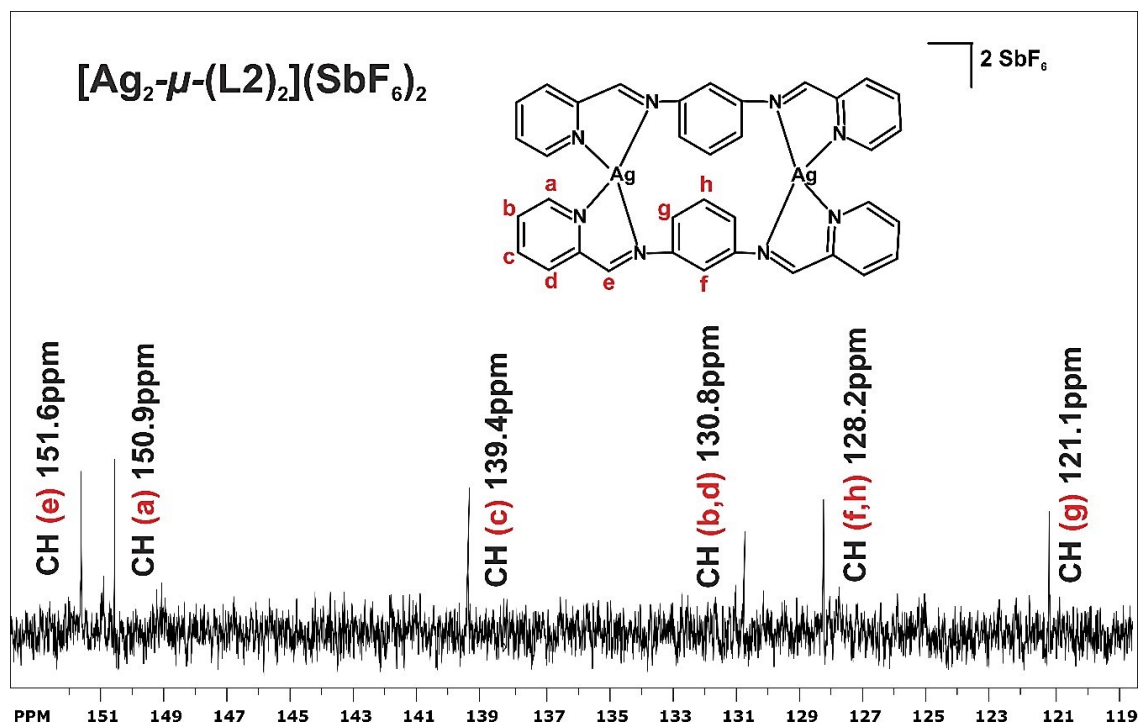


Figure S4: Assigned <sup>13</sup>C NMR spectrum of [Ag<sub>2</sub>-μ-(L2)<sub>2</sub>](SbF<sub>6</sub>)<sub>2</sub>.

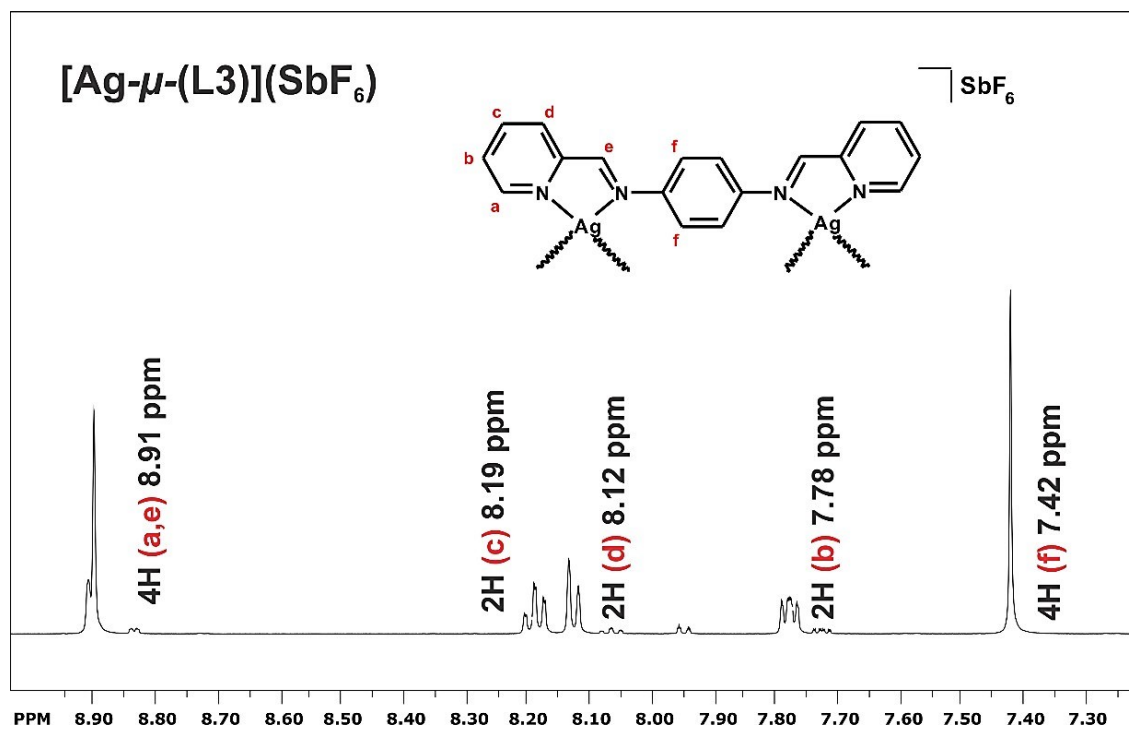


Figure S5: Assigned <sup>1</sup>H NMR spectrum of [Ag-μ-(L3)](SbF<sub>6</sub>).

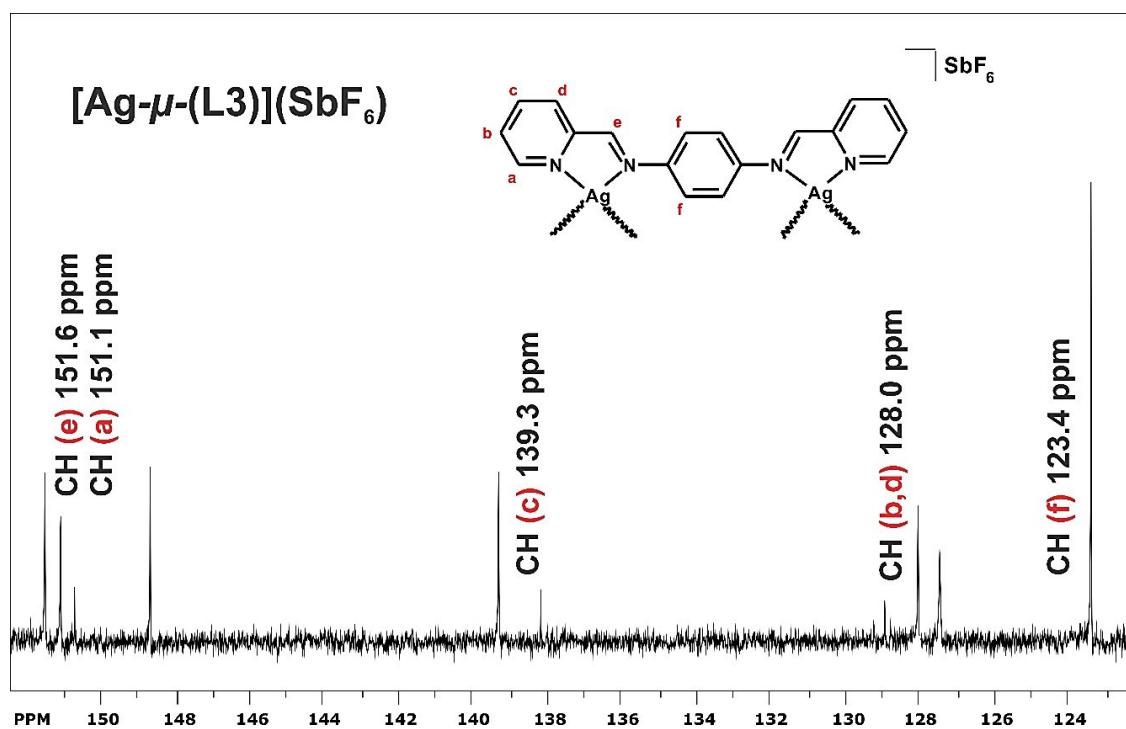


Figure S6: Assigned <sup>13</sup>C NMR spectrum of [Ag- $\mu$ -(L3)](SbF<sub>6</sub>).

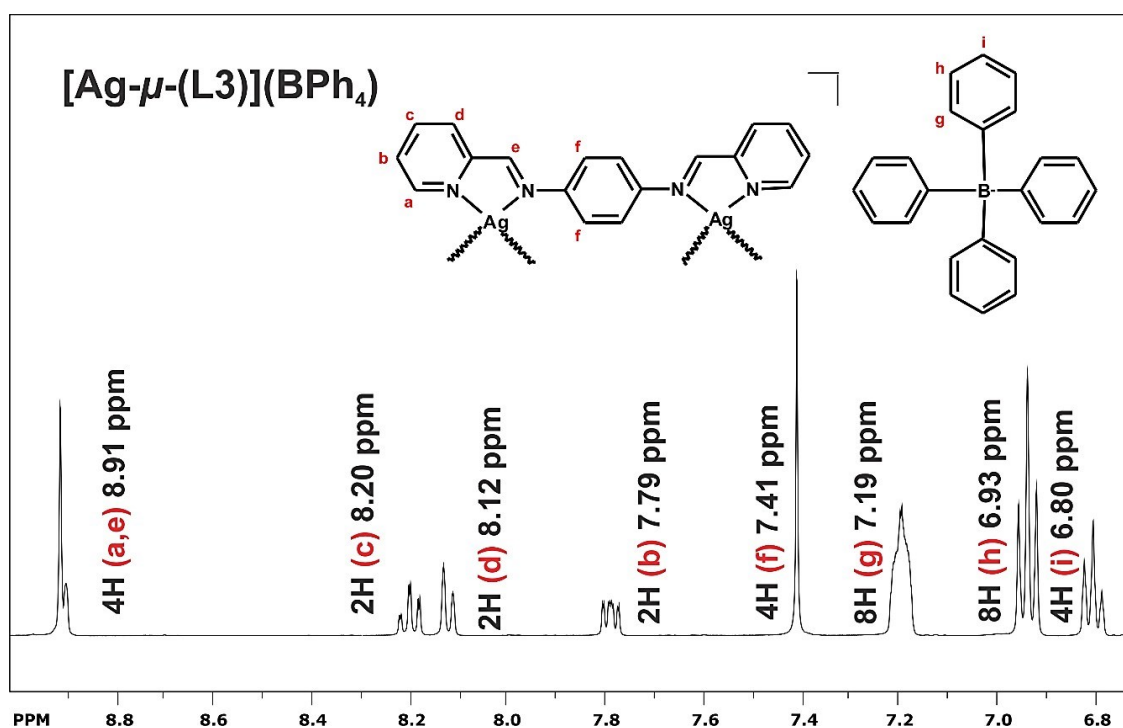


Figure S7: Assigned <sup>1</sup>H NMR spectrum of [Ag- $\mu$ -(L3)](BPh<sub>4</sub>).

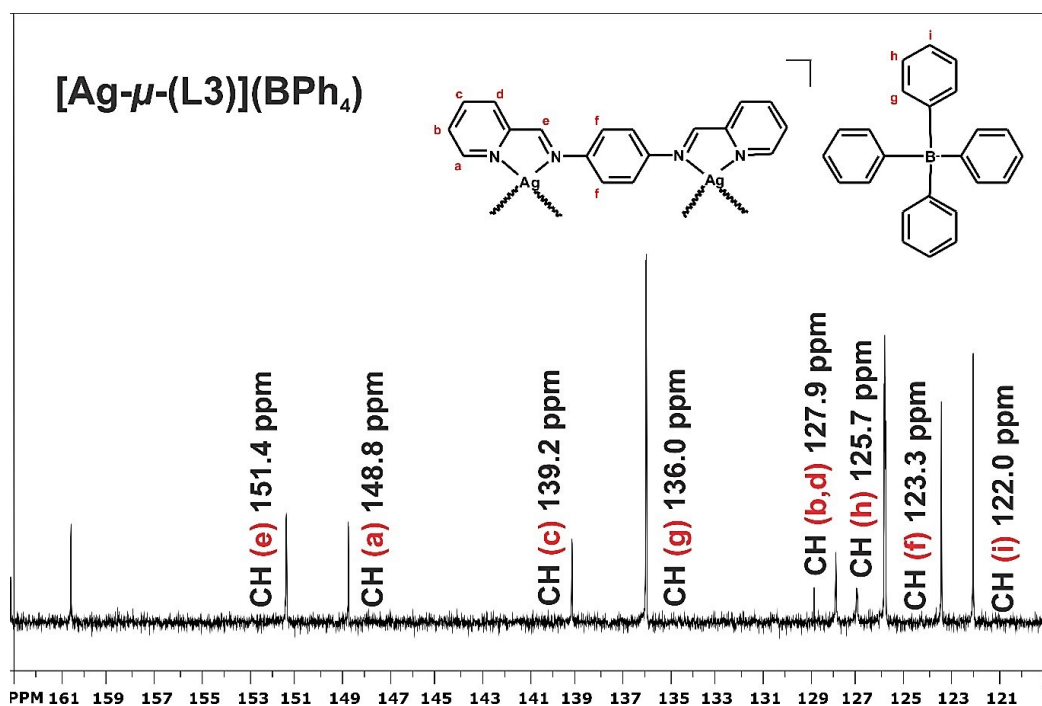


Figure S8: Assigned  $^{13}\text{C}$  NMR spectrum of  $[\text{Ag}-\mu\text{-(L3)}](\text{BPh}_4)$ .

### Synthesis of the free ligand *N,N'*-bis[(*E*)-pyridin-2-ylmethylidene]benzene-1,4-diamine

To a clean and dry round bottomed flask was added 1,4-phenylenediamine (2.73 g, 25.2 mmol) and pyridine-2-carbaldehyde (5.41 g, 50.5 mmol) and acetonitrile (60 mL). The sample was heated to reflux for 60 minutes, during this time a bright yellow precipitate formed. The precipitate was separated from the reaction mixture by gravity filtration and washed with acetonitrile until the filtrate was colourless. The sample was then washed once with diethylether (20 mL) and allowed to air dry. The final yield was 5.84 g, 81%.  $^1\text{H}$  NMR (400 MHz,  $\text{DMSO}-d_6$ , 303K) [ $\delta$ , ppm]: 7.46 (s, 4H,  $\text{N}_{\text{im}}\text{CCH}$ ), 7.55 (m, 2H,  $\text{N}_{\text{py}}\text{CHCH}$ ), 7.98 (t of d, 2H,  $\text{N}_{\text{py}}\text{CCHCH}$ ), 8.19 (d, 2H,  $\text{N}_{\text{py}}\text{CCH}$ ), 8.67 (s, 2H,  $\text{N}_{\text{im}}\text{CH}$ ), 8.74 (d, 2H,  $\text{N}_{\text{py}}\text{CH}$ ).

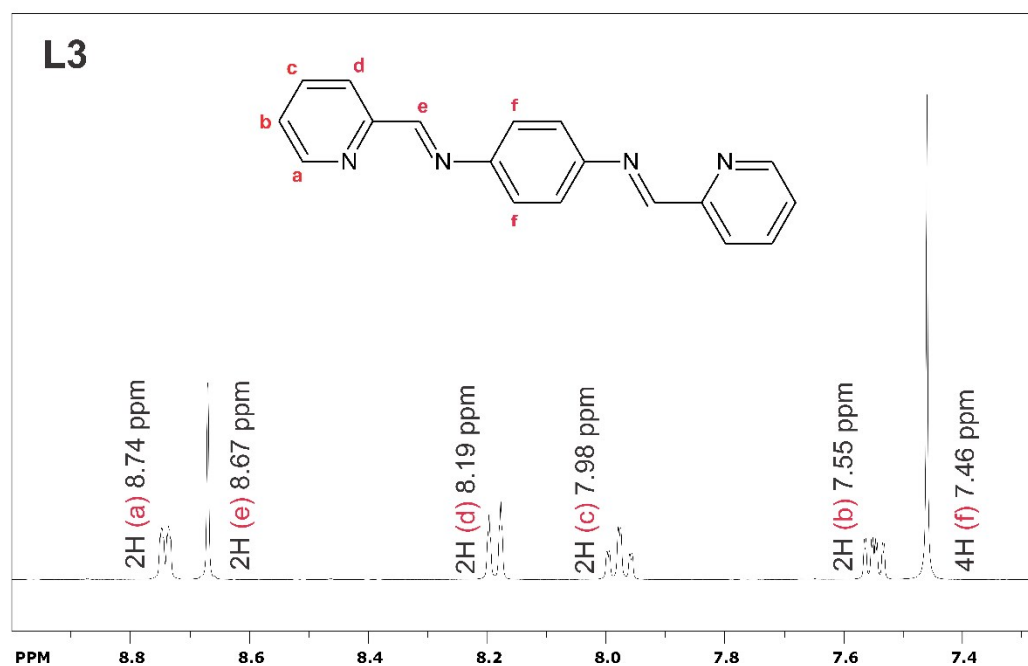


Figure S9: Assigned  $^1\text{H}$  NMR spectrum of (L3).

## Spectroscopic NMR titration

4.0 mg of L3 was dissolved in DMSO-d<sub>6</sub> (0.5 mL) and the <sup>1</sup>H NMR spectrum recorded and referenced according to the residual protonated DMSO at 2.50 ppm. A second solution of AgSbF<sub>6</sub> was prepared by dissolving 4.8 mg (1 molar equivalent) in DMSO-d<sub>6</sub> (0.5 mL). A 0.5 molar equivalent of AgSbF<sub>6</sub> (0.25 mL of the stock solution) was added to the free ligand and <sup>1</sup>H NMR spectrum recorded after a 5-minute incubation period at room temperature. A second aliquot comprising 0.5 molar equivalents was then added to give a 1:1 metal:ligand ratio and the <sup>1</sup>H NMR spectrum recorded after a 5-minute incubation period. The three spectra are shown in Figure S10.

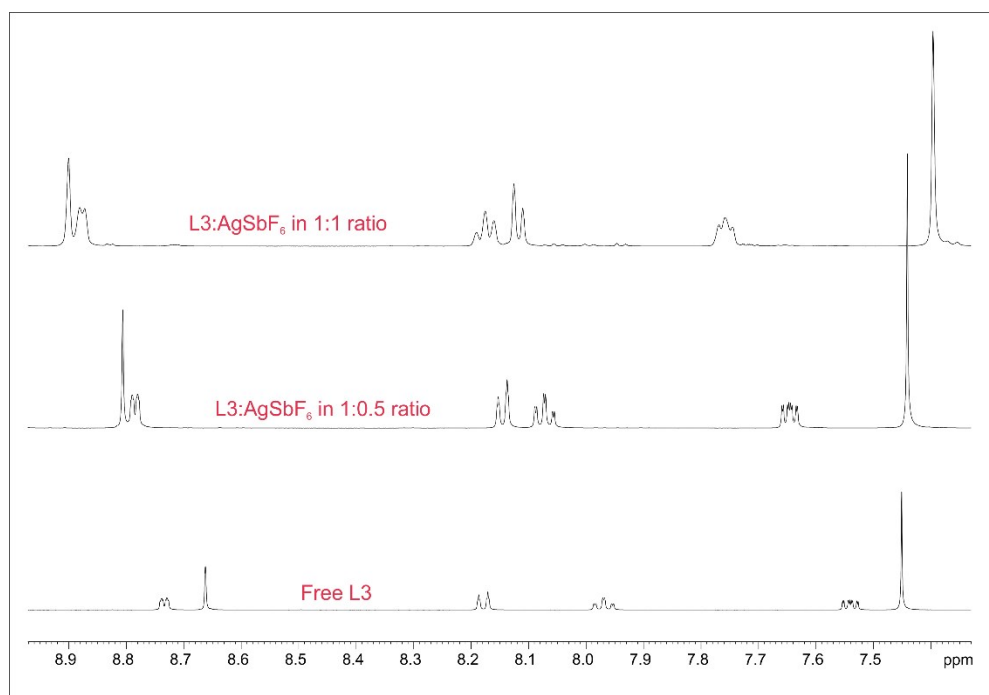


Figure S10: The change in <sup>1</sup>H NMR chemical shift of the ligand with varying ratios of AgSbF<sub>6</sub> in DMSO-d<sub>6</sub>. Note that the imine C–H and α-pyridyl C–H switch positions upon chelation to the metal ion. Although the chemical shifts of both move downfield, the imine C–H moves further downfield, past the chemical shift for the α-pyridyl C–H. These spectra show that metal ion chelation occurs in solution, and it is likely that the species observed in the solid state is also found in the solution state. Due to the electron withdrawing effects of the metal ion, the chemical shifts of all hydrogen atoms move downfield (de-shielded by the electron withdrawing effects). The chemical shifts for the spectrum with a 1:1 metal:ligand ratio match those observed when a crystalline sample of [Ag-μ-(L3)](SbF<sub>6</sub>) is dissolved in DMSO-d<sub>6</sub>.

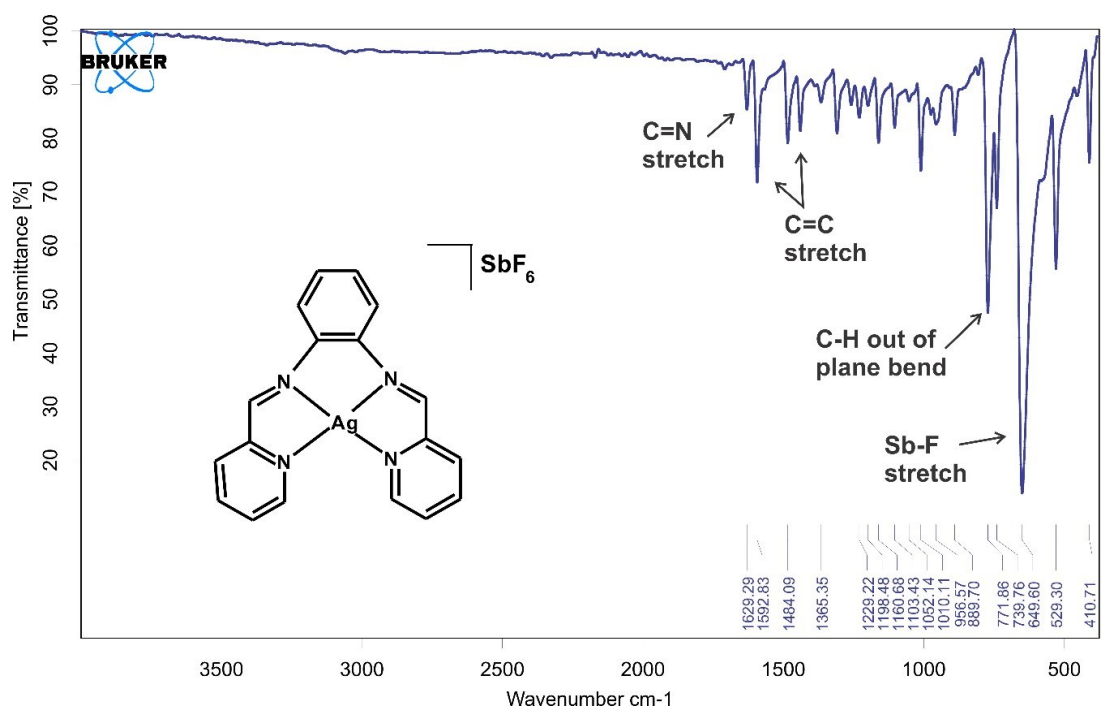


Figure S11: Assigned IR spectrum of [Ag(L1)](SbF<sub>6</sub>).

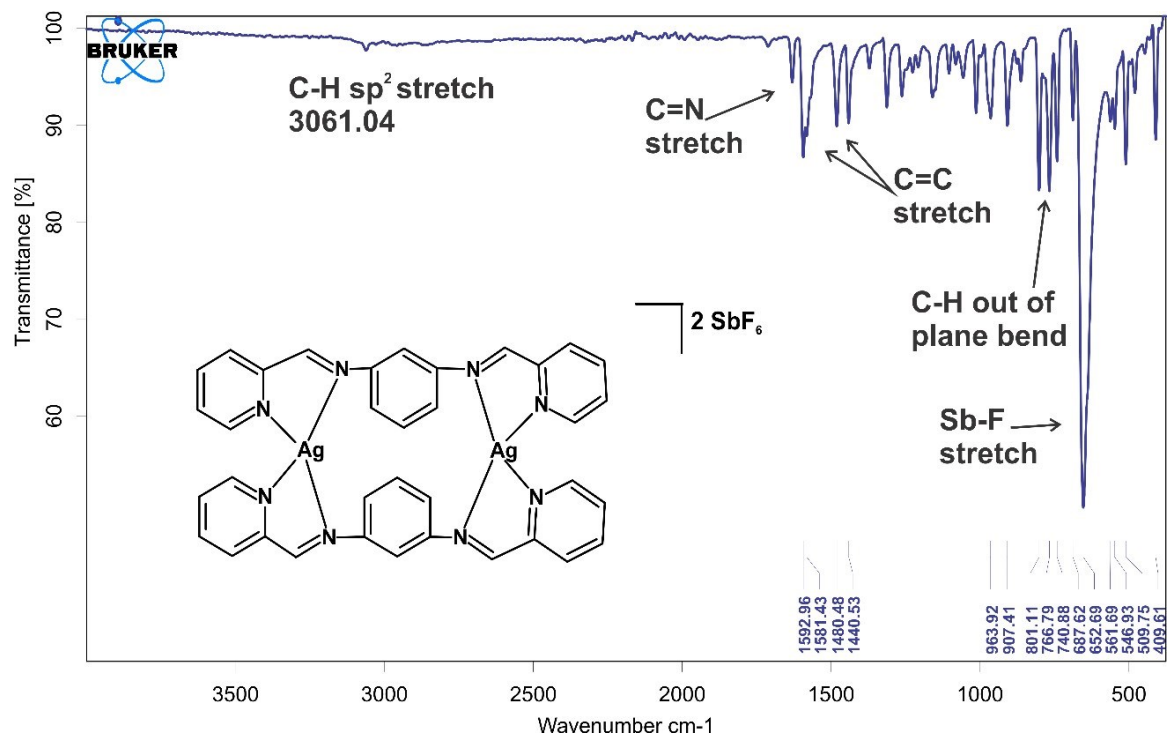


Figure S12: Assigned IR spectrum of [Ag<sub>2</sub>-μ-(L2)<sub>2</sub>](SbF<sub>6</sub>)<sub>2</sub>.

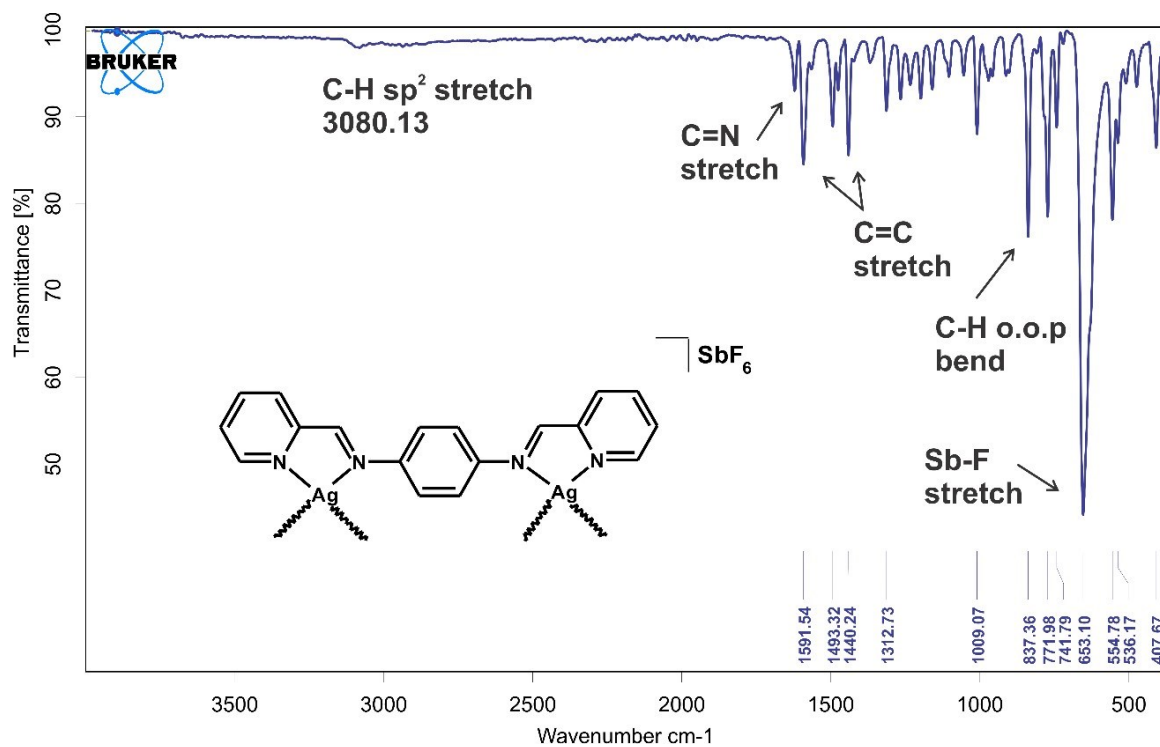


Figure S13: Assigned IR spectrum of  $[\text{Ag}-\mu\text{-(L3)}](\text{SbF}_6)$ .

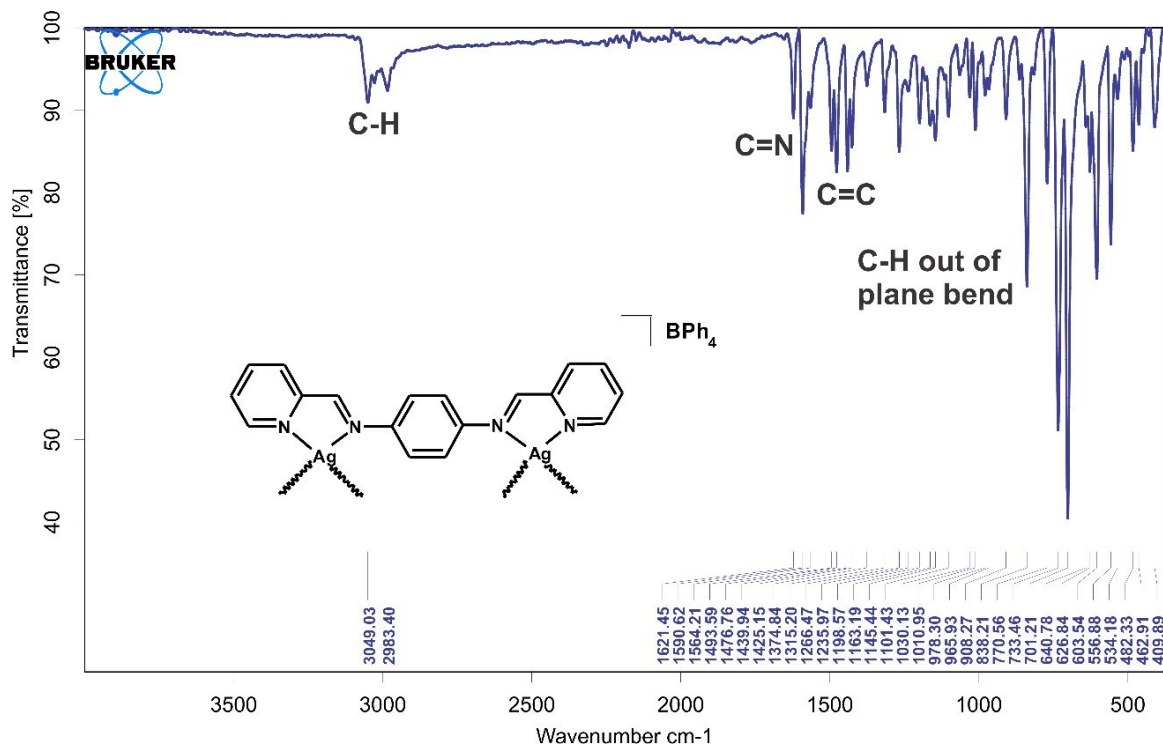
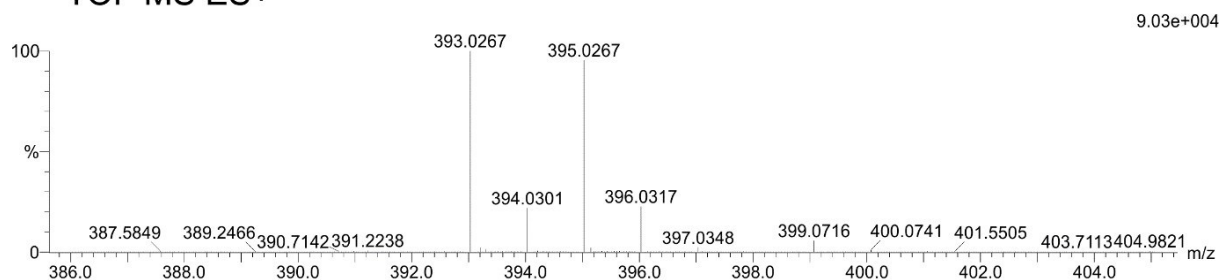


Figure S14: Assigned IR spectrum of  $[\text{Ag}-\mu\text{-(L3)}](\text{BPh}_4)$ .



### TOF MS ES+

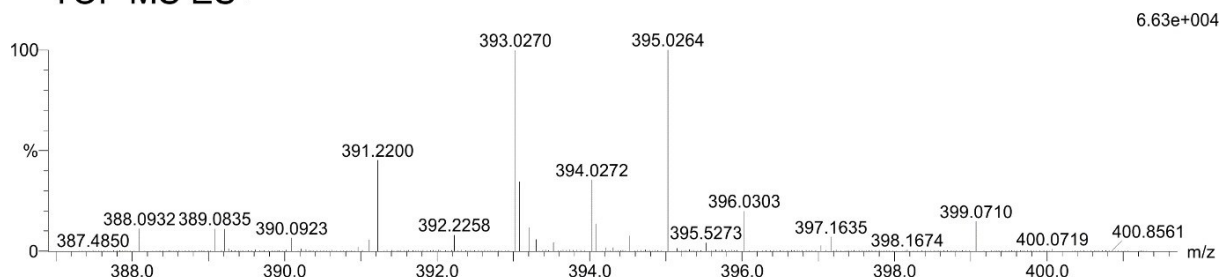


Minimum: -1.5  
Maximum: 5.0 500.0 100.0

Mass	Calc. Mass	mDa	PPM	DBE	i-FIT	i-FIT (Norm)	Formula
393.0267	393.0269	-0.2	-0.5	13.5	509.2	0.0	C18 H14 N4 Ag

Figure S15: ESI-MS spectrum of  $[Ag(L1)]^+$  showing the molecular ion peak.

### TOF MS ES+

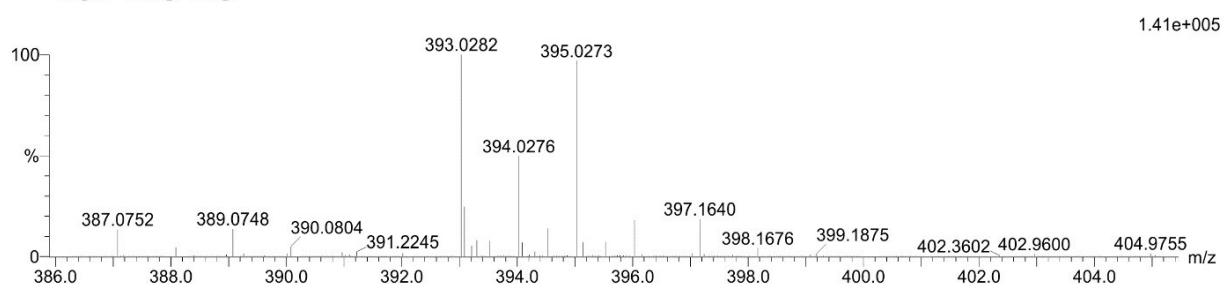


Minimum: -1.5  
Maximum: 5.0 500.0 100.0

Mass	Calc. Mass	mDa	PPM	DBE	i-FIT	i-FIT (Norm)	Formula
393.0270	393.0269	0.1	0.3	13.5	566.3	0.0	C18 H14 N4 Ag

Figure S16: ESI-MS spectrum of  $[Ag_2-\mu-(L_2)_2]^{2+}$  showing the molecular ion peak.

### TOF MS ES+



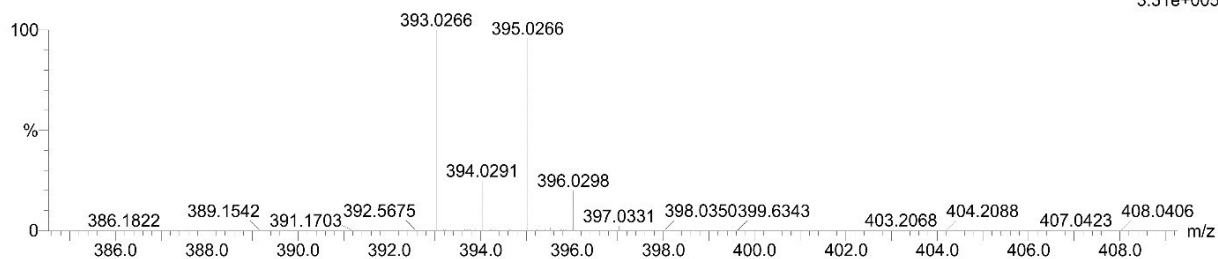
Minimum: -1.5  
Maximum: 5.0 500.0 100.0

Mass	Calc. Mass	mDa	PPM	DBE	i-FIT	i-FIT (Norm)	Formula
393.0282	393.0269	1.3	3.3	13.5	574.5	0.0	C18 H14 N4 Ag

Figure S17: ESI-MS spectrum of  $[Ag-\mu-(L_3)]^+$  showing the molecular ion peak. Sample with an  $SbF_6^-$  anion.

# TOF MS ES+

3.31e+005



Minimum: -1.5  
Maximum: 5.0 50.0 100.0

Mass	Calc. Mass	mDa	PPM	DBE	i-FIT	i-FIT (Norm)	Formula
393.0266	393.0269	-0.3	-0.8	13.5	603.1	0.0	C18 H14 N4 Ag

Figure S18: ESI-MS spectrum of  $[\text{Ag}-\mu\text{-(L3)}]^+$  showing the molecular ion peak. Sample with an  $\text{BPh}_4^-$  anion.

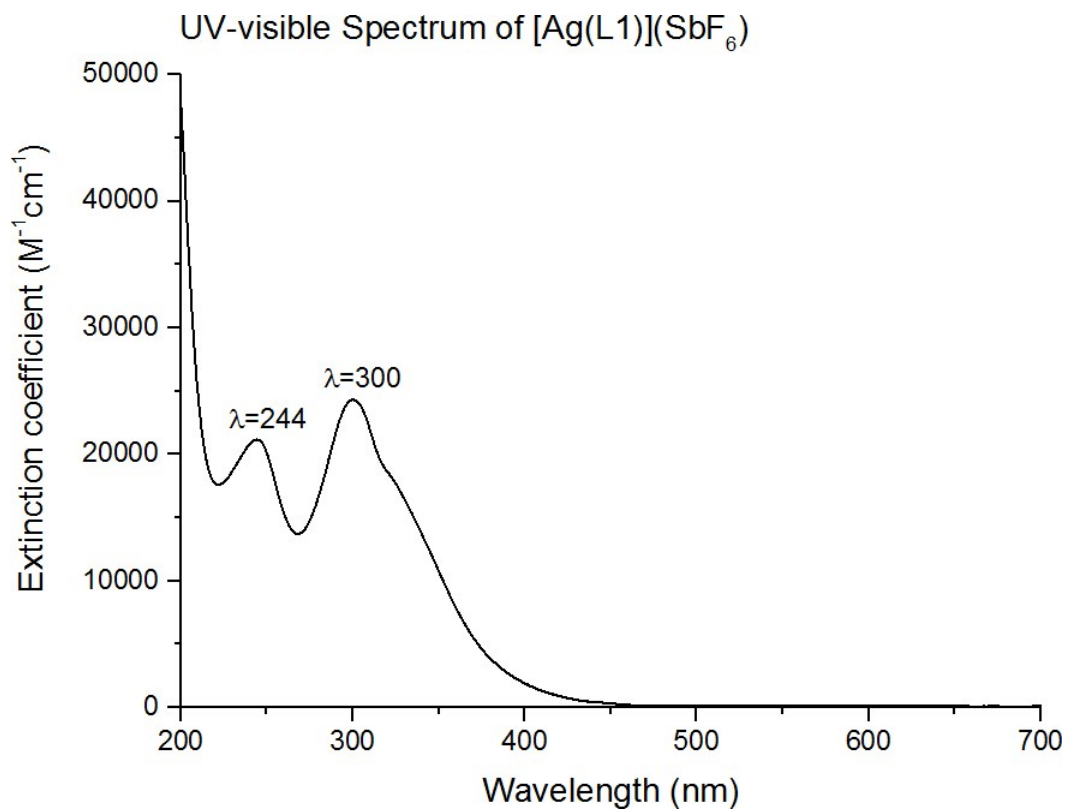


Figure S19: UV-visible spectrum of  $[\text{Ag(L1)}]\text{SbF}_6$ . The spectrum was recorded in acetonitrile.

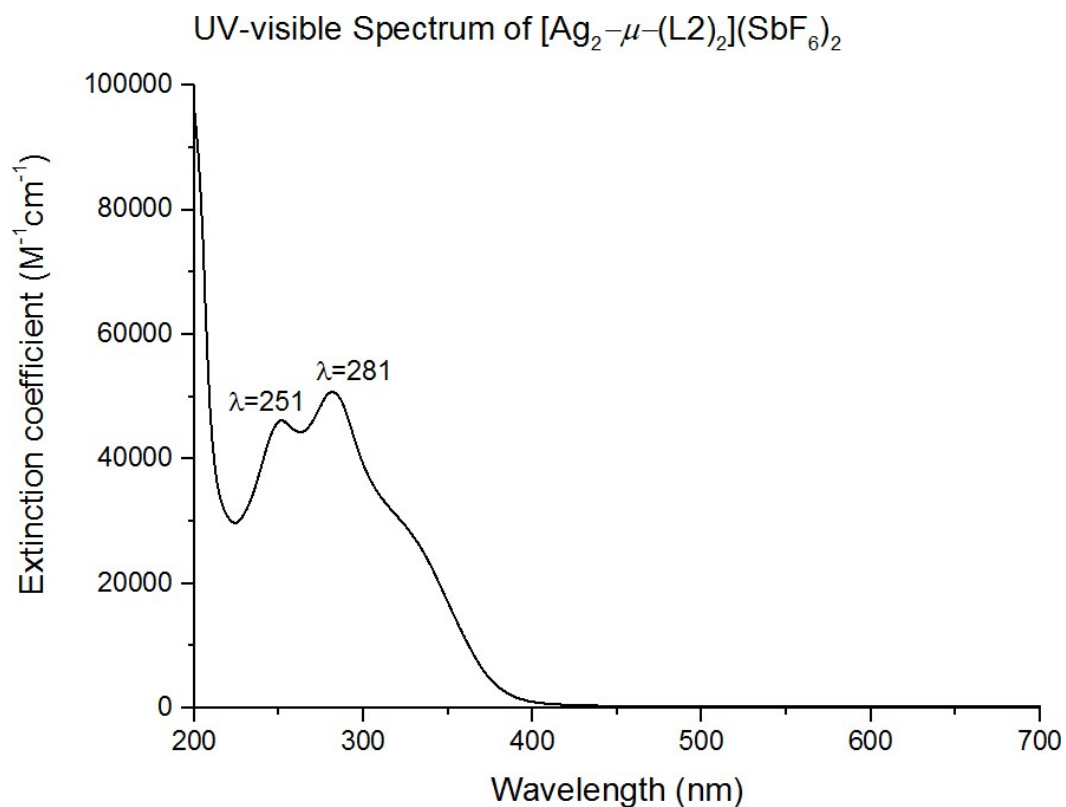


Figure S20: UV-visible spectrum of  $[\text{Ag}_2-\mu-(\text{L}2)]_2(\text{SbF}_6)_2$ . The spectrum was recorded in acetonitrile.

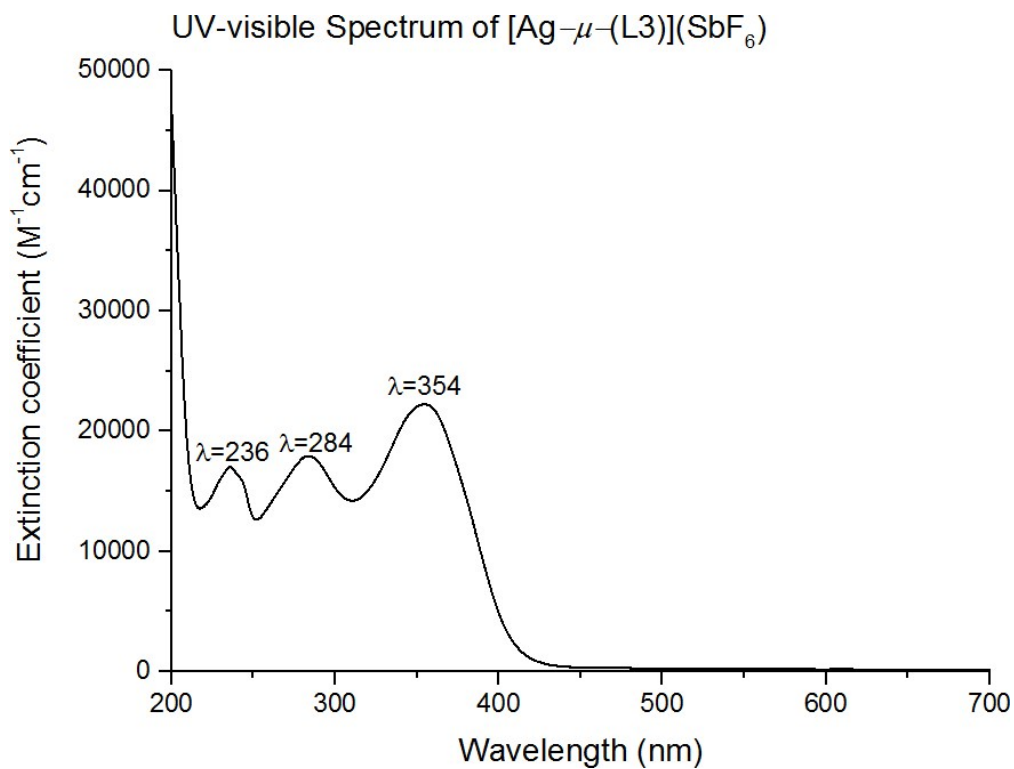


Figure S21: UV-visible spectrum of  $[\text{Ag}-\mu-(\text{L}3)](\text{SbF}_6)$ . The spectrum was recorded in acetonitrile.

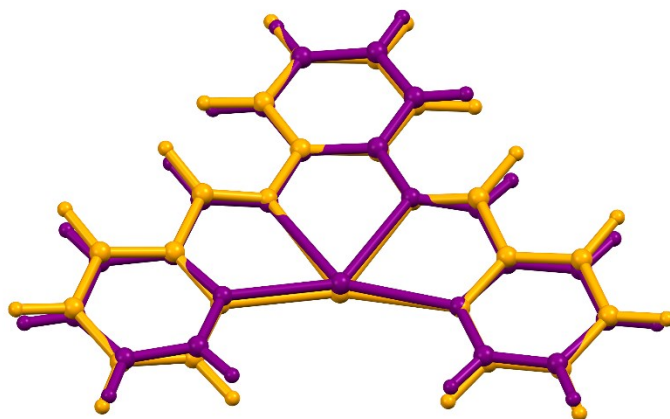


Figure S22: Least-Squares fit of the geometry-optimised (yellow) and experimental (purple) structures of  $[\text{Ag}(\text{L1})](\text{SbF}_6)$  showing good correlation between the structures (RMSD = 0.1814 Å). The rigidity of the ligand and few degrees of freedom allow for the structure to be accurately simulated *in vacuo*. The intermolecular interaction in the solid state have little influence on the molecular geometry.

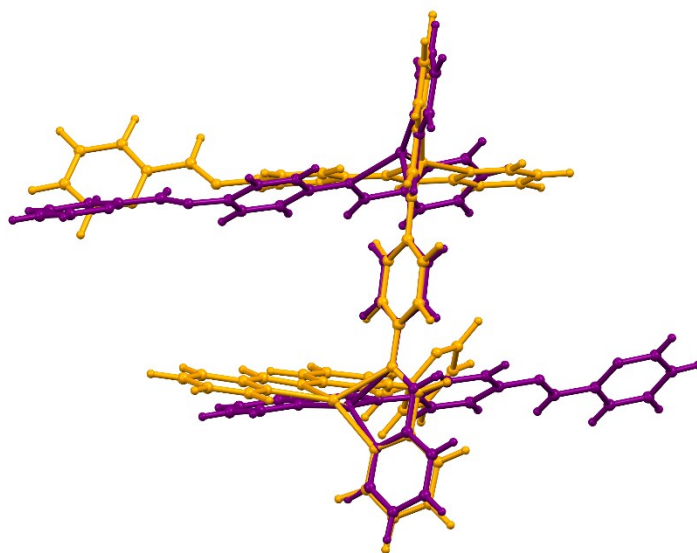


Figure S23: Least squares fit of a trimeric portion of the polymer  $[\text{Ag}-\mu-(\text{L3})]^{2+}$ . Only the bridging ligand was used in the least squares fit. The structure shows that in the absence of steric restraints imposed by the crystal lattice, the geometry-optimised (yellow) structure has the ligands subtending an angle of *ca.* 90°.

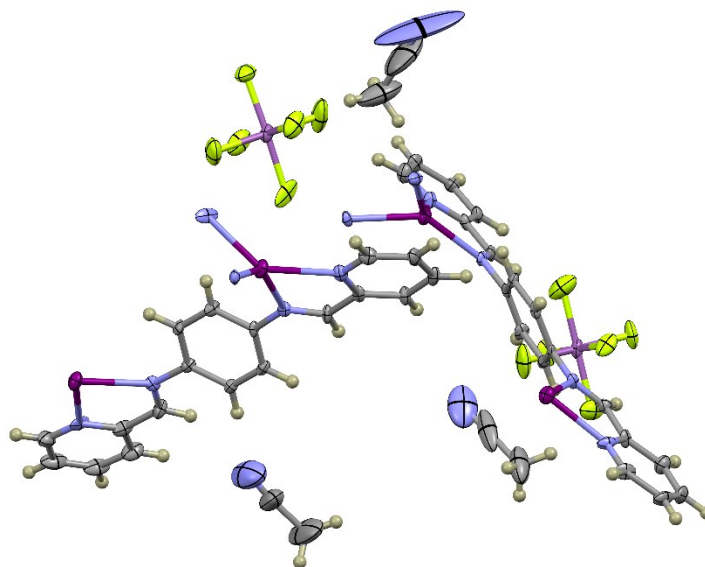


Figure S24: Structure of  $[\text{Ag}-\mu\text{-(L3)}](\text{SbF}_6)$  shown with 50% probability surfaces. The solvent in the lattice has been resolved and shows three acetonitrile molecules with low site occupancy values. The crystallographic data are shown in Table S1.

Table S1: Summary of crystal data and structure refinement details for  $[\text{Ag}-\mu\text{-(L3)}](\text{SbF}_6)$  with the solvent in the lattice resolved.

Crystal Data	$[\text{Ag}-\mu\text{-(L3)}](\text{SbF}_6)$
Chemical Formula	$\text{C}_{24}\text{H}_{23}\text{AgF}_6\text{N}_4\text{Sb}$
Molar Mass $\text{g mol}^{-1}$	753.10
Crystal system, space group	Monoclinic, $P2_1/c$
a, b, c / Å	13.6966(13), 13.1588(12), 26.895(3)
$\beta$ °	$\beta = 96.078(4)$
Temperature / K	100(2)
Z	4
V / Å <sup>3</sup>	4820.1(8)
F (000)	2416
$\mu$ / mm <sup>-1</sup>	2.00
Crystal Dim. / mm	0.21 × 0.08 × 0.01
<b>Data Collection</b>	
Total, unique data	34605, 11340
$R_{\text{int}}$	0.041
<b>Refinement</b>	
Final R indices, [ $I > 2\sigma(I)$ ]	$R_1 = 0.098$ , $wR_2 =$ 0.195

The data in the table above show a less satisfactory model than that achieved through the use of Platon SQUEEZE. Hence the other model was selected for the main manuscript.